A framework for P-cycle assessment in wastewater treatment plants

Vedran Vučić, Christine Süring, Hauke Harms, Susann Müller*, Susanne Günther

Helmholtz Centre for Environmental Research – UFZ, Department Environmental Microbiology, Permoserstrasse 15, 04318 Leipzig, Germany

Corresponding author:
*Susann Müller, Helmholtz Centre for Environmental Research – UFZ, Permoserstrasse 15, 04318 Leipzig, Germany, email: susann.mueller@ufz.de

ABSTRACT

Phosphorus (P) in wastewater has a variety of negative effects and is usually permanently lost as a non-renewable resource. To mitigate future P shortage, P must be recovered from wastewater, preferably by bio-based technologies to avoid toxic side streams. A standardized procedure for the determination of P types and P concentrations in all liquid and solid process stages was established, which is applicable to all full-scale wastewater treatment plants (WWTP). Based on this, an equally universal calculation framework for P-cycle assessment based on volume flow and mass load rates was designed to identify the most promising process streams for biological P recovery. As an example, in 16 process streams of a typical WWTP concentrations of free, bound and total P were calculated and microbial communities were analyzed by flow cytometry over 748 days. The most promising process streams for the recovery of free P were anaerobic digester sludge, centrate and the water-extracts of the biosolids with 0.510 kg P m^{-3}, 0.075 kg P m^{-3} and 1.023 kg P m^{-3}, while the best process streams for the recovery of bound P were return sludge, excess sludge, and the solids of the biosolids with 0.300 kg P m^{-3}, 0.268 kg P m^{-3}, and 1.336 kg P m^{-3}, respectively. Microorganisms capable of P accumulation were active in all process stages and it was observed that chemical P precipitation antagonizes biological P removal. The framework for P-cycle assessment was able to identify process streams that are economically viable to make future in-stream technologies for biological P removal feasible.

KEY WORDS: phosphorus, biological phosphorus recovery, phosphorus accumulation, calculation of process streams, microbial community flow cytometry, microbial community

1 INTRODUCTION

Phosphorus (P) is one of the building blocks of life on earth and is essential for the functioning of cell membranes, energy transfer or DNA synthesis. There is no chemical component that can substitute P in the life cycle, and therefore P is irreplaceable (Cordell et al., 2009). In addition to the natural P cycle of about 10 Mt a^{-1} of P, there is also an anthropogenic P cycle, which covers mostly fertilizers in agriculture, compounds in the chemical and pharmaceutical industries, and human waste. 28.6 Mt a^{-1} P is mined from the finite amount of phosphate rock (68,776 Mt; 9,005 Mt as P) for anthropogenic needs. Humanity currently loses P at all stages of the P production system (Daneshgar et al., 2018) and about 100 % of the P absorbed from food (3.7 Mt) (Kok et al., 2018) is discharged via wastewater (Cordell et al., 2009), where it is lost.

As a non-renewable resource, P is classified by the European Commission as a critical raw material (COM, 2017). Efforts are therefore being made worldwide to recover P from wastewater and associated streams. Among several European countries operating at national level, the Swiss Ordinance on Waste Avoidance and Disposal requires the recovery of P not only from wastewater, sewage sludge, and sewage sludge ash, but from 2026 onwards also from P in meat and bone meal (Mehr et al., 2018). In Germany, the Sewage Sludge Ordinance (SSO) (AbfKlärV, 2017) makes the recovery of P from sewage sludge mandatory. After a transitional period of 15 years, all wastewater treatment plants (WWTP) with a size > 50,000 population equivalents will be obliged to recover P if the values exceed 20 g P per kg sewage sludge dry matter. This will force about 500 largest out of the 9,300 German WWTPs, which treat 2/3 of the wastewater, to install suitable technologies for P recovery. Sweden and Austria are on the same path with the proposal to make P recovery from sewage sludge compulsory or to achieve specific P recycling rates (Günther et al., 2018). Poland is also expected to follow this example in the frame of its circular economy plan (Smol, 2019).

WWTP process streams with a P concentration above 0.05 kg m^{-3} are considered economically feasible for P recovery (Cornel and Schaum, 2009) and could include all liquid and solid phases of the wastewater as well as sludge ash (Shaddel et al., 2019; Nattorp et al., 2017; Desmidt et al., 2015). The most common full-scale recovery technologies currently in use are those which precipitate free P from liquid phases as magnesium ammonium phosphate (MAP, 4 out of 10 plants) or MAP/calcium phosphate minerals (2 out of 10 plants) (Law and Pagilla, 2018). These technologies avoid problems with toxic waste streams and costly technological facilities encountered when using P recovery based on solid sludge or ash (Li et al., 2019). However, they are dependent on the addition of Mg, which is also part of the critical list of raw materials and has the same high supply risk and an even greater economic importance than P (COM,

2017). Instead, upcoming biological based recovery technologies that operate without chemical additives can easily provide P for down-stream applications by using microorganisms (Ma et al., 2018) or algae (Orfanos and Manariotis, 2019). To prevent the loss of P due to inefficient biological P recovery strategies, it is necessary to identify process stages where biological P removal would be feasible and which have the potential to be applied on-spot and selectively.

P is accumulated by microorganisms as part of the biomass and as polyphosphates (polyP). The accumulation of polyP is a universal trait and leads to values of up to 4 -5 % of sludge dry matter (Blackall et al., 2002). The efficiency of microorganisms to accumulate or release P in the successive process streams of a WWTP depends on various parameters such as oxygen availability, carbon concentration or community composition (Ahn et al., 2007). To what extent microorganisms contribute to P accumulation in the different process streams and how their respective capacity for P accumulation could be influenced by chemical P precipitation techniques has not been investigated to date.

In WWTPs, the analysis of the P contents is required by the law only for the inflow and outflow. Other streams are monitored less frequently or not at all, so that the respective P types and contents of P are often not considered. In addition, P types are still measured as different forms and calculated in hardly comparable units, as shown by examples in SI Table 1, although EU and ISO standards are available to support a global comparison of values (Cieślik and Konieczka, 2017). The currently most frequently used analytical methods for the determination and description of P-types are listed in SI Table 2. There seems to be a need for a unified approach to the calculation of P contents and forms in all stages of a WWTP to enable decision making on P recovery strategies.

In this study, we aim i) to establish a framework for P-cycle assessment for all process streams in a full-scale WWTP considering all volume flow and mass load rates, ii) to calculate P values based on EU ISO standards for P determination and to establish free P and bound P as most relevant P types in a WWTP, iii) to assess the degree of involvement of the microorganisms in P accumulation and their P accumulation capacity in the different process streams, and finally, iv) to highlight process streams where the establishment of on-site interfaces for biological P recovery would be economically feasible.

2 MATERIAL AND METHODS

2.1 WWTP process streams

Samples were obtained from the WWTP Eilenburg (51°28'29.7"N; 12°37'13.9"E, Germany), which treats the wastewater of 49,000 inhabitants, i.e. up to 5,000 m^3 per day. P is mainly removed by biological P elimination, but chemical precipitation is used as a back-up to ensure discharge limits according to the German Wastewater Ordinance (AbwV, 2020). The scheme of the Eilenburg WWTP with the corresponding process streams and the 16 sampling points is shown in Figure 1: inflow (1.inflow), grit chambers (2.grit chamber start, 3.grit chamber end) and primary clarifier (4.primary clarifier). In the primary clarifier the primary sludge (5.primary sludge) is separated and pumped to meet the thickened excess sludge (12.excess sludge) before both sludges are fed into the anaerobic digester. From 4.primary clarifier, wastewater is pumped into the aeration tanks (6.aeration tank1, 7.aeration tank2). From there, wastewater goes to the precipitation shaft (8.precipitation shaft) for chemical P removal if necessary. Following, processed wastewater reaches the secondary clarifiers (9.secondary clarifier1, 10.secondary clarifier2), and the effluent (16.effluent). Settled sludge from the secondary clarifiers is partly returned to the aeration tanks as return sludge (11.return sludge, approx. 96.4 % of the volume load rate of settled sludge), and partly as 12.excess sludge (approx. 3.6 % of the volume load rate of settled sludge; this value was used to determine 11.return sludge of the last 4 sampling days, which could not obtained for operational reasons) into the anaerobic digester after being thickened with a polymer. After digestion, 13.anaerobic digester sludge is dewatered and divided into 15.biosolids and 14.centrate, which is recirculated to the 6. and 7.aeration tanks1,2. Hydraulic retention time for sampling points 1-7, 9- 12 and 14-15 is less than 24 h. Hydraulic retention time of 13.anaerobic digester sludge is around 30 d.

2.2 Samplings and measurements

Within a time frame of 748 days, 45 sampling campaigns including 16 sampling points were performed. Some sampling points were less frequently available for sampling due to operational issues. The number of samples were as follows: 1.inflow (n= 45), 2.grit chamber start (n= 44), 3.grit chamber end (n= 45), 4.primary clarifier (n= 44), 5.primary sludge (n= 11), 6.aeration tank1 (n= 45), 7.aeration tank2 (n= 45), 8.precipitation shaft (n= 45), 9.secondary clarifier1 (n= 44), 10.secondary clarifier2 (n= 44), 11.return sludge (n= 16), 12.excess sludge (n= 39), 13.anaerobic digester sludge (n= 42), 14.centrate (n= 44), 15.biosolids (solids n= 42, water-extracts n= 42), 16.effluent (n= 44). A total of 681 samples were analyzed for abiotic data such as dry matter (DM), total P, bound P and free P. Cytometric data were obtained from 465 samples of the total data set and the abundances of cells were measured within 68 gates per sample

(= subcommunities, SC). A total of 31,620 SC data were used for bioinformatics analyses (SI Table 3). All samples (sampling points 1-14, 16) were taken from the upper third of the respective process stream using a manual 1 L sampler. Before a sample was taken, the sampler was rinsed with the sample medium at least once. For the process stream 15.biosolids about 0.5 kg of fresh material was taken from the container, which was then thoroughly mixed and further treated as described below. Sampling was always done at the same time and sequence of sampling points. Sample preparations began immediately after sampling for all analyses.

2.3 Analyses

2.3.1 Determination of total P and free P

Of all samples 1-14 and 16, both the liquid and the solid phases were included in the analyses. For the P analysis method, about 0.5 mL per sample were taken and diluted, depending on the expected concentration. The total P concentration was determined with the Phosphate 15 kit (Macherey-Nagel GmbH & Co. KG, Düren, Germany) according to a standard method (DIN EN ISO 6878:2004-09). The samples were digested with the Nanocolor Vario C2 heating block (Macherey-Nagel GmbH & Co. KG, Düren, Germany) for 30 min at 120 °C to release biologically and chemically bound P. After digestion, the samples were treated until formation of phosphorus molybdenum blue as the end product, the concentration of which was measured spectrophotometrically as *ortho*-P. The free P concentration of the samples was determined by centrifugation of the whole samples at 3,200 g at 4 °C, 10 min (Eppendorf Centrifuge 5804 R, Hamburg, Germany) and by using only the supernatant with the same Phosphate 15 kit. These data were measured from the concluding 11 days of sampling and the other data were assessed on the basis of the obtained average. In this study, all values of *ortho*-P were calculated as elemental total P ($\gamma\ (P)_{TP}$, kg m^{-3}) or elemental free P ($\gamma\ (P)_{FP}$, kg m^{-3}) with a conversion factor of 3.07 for PO_4^{3-} to P (Macherey-Nagel). In 15.biosolids, P was determined in 0.5 g biosolids suspended in 4.5 mL bidistilled water for 10 min, during which the sample was homogenized by vortexing (PV-1 Vortex Mixer, Grant Instruments, Cambridgeshire, UK). Afterwards, the total P in the whole sample was determined. The free P was analyzed after centrifugation in the supernatant as before. Bound P is calculated as indicated in (Eq 1) except for 15.biosolids. Here, the bound P in dry matter was measured by an accredited external laboratory by a standard method (DIN EN ISO 17294-2, via ICP-MS). The total P, the free P and the bound P values were used to calculate the respective P mass load rates of the WWTP process streams (Eq 14 - 16).

2.3.2 Determination of dry matter (DM)

The DM measurement was done for all samples for which P concentrations were determined (SI Figure 1). The samples were collected in 50 mL or 15 mL Falcon tubes depending on biomass density and centrifuged at 3,200 × g for 10 min at 4 °C (Eppendorf Centrifuge 5804 R, Hamburg, Germany), and the supernatant was discarded. The pellets were transferred to 2 mL Eppendorf tubes and centrifuged a second time at 6,000 × g for 10 min at 4 °C (Thermo Scientific Fresco 21, Langenselbold, Germany). All initial volumes of samples are listed in SI Table 3. After the second centrifugation step the supernatant was discarded and the pellet dried for 3 d at 50 °C. The DM was determined using the Sartorius BP 110 balance (Göttingen, Germany) and the values corrected to the sample volumes (Eq 2). The value of (Eq 2) was used to calculate the P content in DM (Eq 3). The procedure was performed in triplicates.

2.3.3 Determination of density in liquid and solid process streams

The density (ρ, kg m^{-3}) (Eq 4) of samples of liquid and solid process streams was measured to enable conversions from volume load rates to mass load rates and *vice versa*. The density was calculated as average values in a 100 mL graduated cylinder, which was weighed after filling with the respective process stream sample (SI Table 3). The density value of 15.biosolids was defined according to Spellman (1996) as 800 kg m^{-3}.

2.4 Flow cytometry measurement of microbiological communities

The samples were fixed in 8 % paraformaldehyde for 30 min at room temperature (RT) with a ratio of 1:4 ($vol_{sample}/vol_{fixative}$) immediately after sampling, with a final concentration of 2 %. After centrifugation (3,200 x g, 10 min, 4 °C) the cells were resuspended in 70 % ethanol and stored at -20 °C (Günther et al., 2016). Staining of the cells was performed as described in Cichocki et al. (2020) and measuring done by flow cytometry. Before measurement, 0.5 µm and 1.0 µm UV Fluoresbrite microspheres (Polysciences, Warrington, PA, USA) were added to the stained cells as an internal marker for measurement accuracy. The samples were analyzed with a prototype CyFlow-Space (Partec, Görlitz, Germany), equipped with a 355 nm laser (Genesis CX355 -60 STM OPS Laser-Diode System, Coherent, CA, USA) and operated at 50 mW. The sample flow rate of the cytometer was 0.5 µL s^{-1} at 1000 events s^{-1}. For each sample 250,000 stained cells were recorded. Bidistilled water was used as sheath fluid and replaced daily. The instrument was calibrated using the same microspheres as above and a DAPI stained bacterial standard with known DNA-pattern. All raw data can be accessed at the FlowRepository (https://flowrepository.org/) under accession numbers FR-FCM-Z2QU and FR-FCM-Z2TP. After generating a cell gate to exclude beads and

noise, 68 gates were defined for all recorded samples to create the gate template (SI Figure 2). The evaluation of the gate data was performed with the software FlowJo version 10.6.2 (FlowJo LLC, Oregon, USA). Events in overlapping gates were excluded from analysis by subtracting proportional event numbers. Only gates with an average cell frequency above 1 % were included in correlation analyses of the data. The number of gates meeting this criterion is shown in SI Table 4.

2.5 Bioinformatics analysis

The cytometric data were evaluated with the bioinformatic tools flowCyBar using the R packages "flowCyBar" (Koch et al., 2013), "flowCore" (Hahne et al., 2009), "hexbin" (Car et al., 2019), "vegan" (Oksanen et al., 2015), and "ggplot2" (Wickham, 2016) with R version 3.6.1. (RCoreTeam, 2018). NMDS plots of flowCyBar derived data were created using Bray-Curtis dissimilarities. The centroids in NMDS plots (Figure 3) and the distances between centroid and the sampling points (SI Table 5) were calculated using R packages "tcltk" (RCoreTeam, 2018) and "raster" (Hijmans and van Etten, 2014). Correlations between the gate derived SC and the abiotic parameters were performed as described by Günther et al. (2016) calculating Spearmans ranked order correlation coefficient rho with a significance value $P<0.05$ using the package "Hmisc" (Harrel et. al., 2018). The first correlation value is obtained using the initial 4 sampling days and each rho and *P* value is written into a table. Then the next sampling day is added to the matrix and the correlation done again for the extended data set. This procedure is repeated until all sampling days are part of the correlation matrix. Visualization of individual rho and *P* values was done using heatmaps and the summary as circos plots using R package "circlize" (Gu et al., 2014).

3 The framework of P-cycle assessment

In this study, the EU ISO standard DIN EN ISO 6878 was used to analyze and determine P concentrations of only three different types of P (total P, free P and bound P) to calculate the P mass load rates of 16 process streams both in liquid and solid phases. To enable such an approach a framework for P-cycle assessment was established. Free P and total P concentrations were used to calculate bound P (Eq 1). The daily volume flow rates (Q) were either obtained from the WWTP or calculated (Eq 5 – Eq 13) and were then used to calculate the daily P mass load rate ($\dot{m}$) for free P (Eq 14, 17), total P (Eq 15, 18), and bound P (Eq 16, 19). DM was analyzed (γ(DM)) (Eq 2), and P content in the DM (Eq 3) was calculated for all sampling points except for the 15.biosolids for which the standard DIN EN ISO 17294-2 was used. Values for volume load rates, mass load rates and DM are provided in SI Table 3 and are summarized as average values in SI Table 7 for a period of 748 days.

3.1 P balance calculation on the basis of total P, free P, and bound P

The free and the total *ortho*-P in the sample was measured and calculated as elemental free P ($\gamma\ (P)_{FP}$, kg m^{-3}) and elemental total P ($\gamma\ (P)_{TP}$, kg m^{-3}) (SI Figure 1). Bound P ($\gamma\ (P)_{BP}$, kg m^{-3}) was calculated as the difference between total P and free P as follows:

Eq (1) $$\gamma\ (P)_{BP}[kg\ m^{-3}] = \gamma\ (P)_{TP}\ [kg\ m^{-3}] - \gamma\ (P)_{FP}\ [kg\ m^{-3}]$$

The P concentrations values obtained from this step were used to calculate the P mass load rates, the P removal rates and to investigate interrelations between P concentrations and the structures of the microbial communities in the respective sampling point.

3.2 Calculation of DM and P content in DM

The DM was calculated as mass concentration (γ_{DM}, kg m^{-3}) with regard to initial sample volume (V_{sample}, m^3), and DM (m_{DM}, kg) as follows:

Eq (2) $$\gamma_{DM}\ [kg\ m^{-3}] = m_{DM}\ [kg] / V_{sample}\ [m^3]$$

The P contents in the DM ($P_{DM\ content}$, g P kg_{DM}^{-1}) for sampling points 1.-14. and 16. were calculated using the mass concentration of bound P (γ_{BP}, g m^{-3}) divided with mass concentration of DM (γ_{DM}, kg m^{-3}) as follows:

Eq (3) $$P_{DM\ content}\ [g\ P\ kg_{DM}^{-1}] = \gamma_{BP}\ [g\ m^{-3}] / \gamma_{DM}\ [kg\ m^{-3}]$$

3.3 Calculation of density

To calculate the density (ρ, kg m^{-3}) the following equation was used:

Eq (4) $$\rho\ [kg\ m^{-3}] = m\ [kg] / V\ [m^3]$$

3.4 Calculation of daily volume load rate per sampling point

To assess daily volume (Q, $m^3\ d^{-1}$) and mass ($\dot{m}$, kg d^{-1}) load rates of all the sampling points, daily volume load rate data were 1) acquired directly from the WWTP Eilenburg, 2) assessed as tank volume or 3) calculated as sum or difference from other known process streams (SI Table 6). Furthermore, stream daily volume load rates were used to calculate P mass load rates.

3.5 Calculation of the volume load rate of the primary sludge

To calculate 5.primary sludge volume load rate (Q_5, $m^3\ d^{-1}$), firstly the volume load rate of the thickened excess sludge (Q_{tES}, $m^3\ d^{-1}$) and secondly the volume load rate of the anaerobic digestion feed were required (Q_{feedAD}, $m^3\ d^{-1}$). The volume load rate of the thickened excess sludge (Q_{tES}, $m^3\ d^{-1}$) must be calculated, whereas the volume load rate of the digester feed (Q_{feedAD}, $m^3\ d^{-1}$) was provided by the WWTP operators.

The volume load rate of thickened excess sludge (Q_{tES}, $m^3\ d^{-1}$) was calculated from the volume reduction parameter of the 12.excess sludge (Q_{12}, $m^3\ d^{-1}$) as estimated by Peirce et al. (1998), which was most suitable for this case. Their reduction parameter of the excess sludge was 80 % and resulted in excess sludge with increased DM between 3 % and 5 %. In the WWTP Eilenburg the DM of excess sludge was increased during the monitoring campaign from around 1.3 % to 7 %. The polymer used to thicken excess sludge by binding the water was Reiflock RF600 (Reiflock Abwassertechnik GmbH, Baden-Baden, Germany).

Eq (5) $$Q_{tES}\ [m^3\ d^{-1}] = Q_{12}\ [m^3\ d^{-1}] \times 0.2$$

Lastly, 5.primary sludge volume load rate (Q_5, $m^3\ d^{-1}$) was assessed by subtracting assessed volume load rate of thickened excess sludge (Q_{tES}, $m^3\ d^{-1}$) from the known volume load rate of anaerobic digester feed (Q_{feedAD}, $m^3\ d^{-1}$):

Eq (6) $$Q_5\ [m^3\ d^{-1}] = Q_{feedAD}\ [m^3\ d^{-1}] - Q_{tES}\ [m^3\ d^{-1}]$$

3.6 Calculation of volume load rates of the aeration tanks 1 and 2

The volume load rate for 6. and 7.aeration tank1,2 ($Q_{6,7}$ $m^3\ d^{-1}$, ($Q_6 = Q_7$)) was calculated using the sum of volume load rates of 9. and 10.secondary clarifier1,2 ($Q_{9,10}$ $m^3\ d^{-1}$, ($Q_9 = Q_{10}$)) (Eq 9) and 12.excess sludge as follows (Q_{12}, $m^3\ d^{-1}$):

Eq (7) $$Q_{6,7}\ [m^3\ d^{-1}] = (Q_9\ [m^3\ d^{-1}] + Q_{10}\ [m^3\ d^{-1}] - Q_{12}\ [m^3\ d^{-1}]) / 2$$

3.7 Calculation of the volume load rate of the precipitation shaft

The volume load rate for 8.precipitation shaft (Q_8, $m^3\ d^{-1}$) was calculated as equal to the sum of the volume load rate of 6. and 7.aeration tank1,2 ($Q_{6,7}$ $m^3\ d^{-1}$):

Eq (8) $$Q_8\ [m^3\ d^{-1}] = Q_{6,7}\ [m^3\ d^{-1}] \times 2$$

3.8 Calculation of the volume load rates of the secondary clarifiers 1 and 2

The volume load rate for 9. and 10.secondary clarifier1,2 ($Q_{9,10}$ $m^3\ d^{-1}$, ($Q_9 = Q_{10}$)) was calculated using the volume load rate of 16.effluent (Q_{16}, $m^3\ d^{-1}$) and 11.return sludge (Q_{11}, $m^3\ d^{-1}$) as follows:

Eq (9) $Q_{9,\,10}\,[m^3\,d^{-1}] = (Q_{16}\,[m^3\,d^{-1}] + Q_{11}\,[m^3\,d^{-1}]) / 2$

3.9 Calculation of the volume load rate of the centrate

13.anaerobic digester sludge is transported to the sludge dewatering (digester sludge dewatering $Q_{DSD,}$ $m^3\,d^{-1}$), where it is then divided in two streams: 14.centrate (Q_{14}, $m^3\,d^{-1}$) and 15.biosolids (Q_{15}, $m^3\,d^{-1}$). DSD ($Q_{DSD,}$ $m^3\,d^{-1}$) volume load rate and 15.biosolids (Q_{15}, $m^3\,d^{-1}$) volume load rates were acquired from the WWTP process operators. The mass load rate of 14.centrate ($\dot{m}_{14}$, kg d^{-1}) was calculated from volume load rates of DSD (Q_{DSD}, $m^3\,d^{-1}$) and 15.biosolids (Q_{15}, $m^3\,d^{-1}$), which were converted to mass load rates (Eq 10 – 11). The densities of the DSD (ρ_{DSD}, kg m^{-3}) and the 15.biosolids (ρ_{15}, kg m^{-3}) streams are not similar and were included accordingly:

Eq (10) $\dot{m}_{DSD}\,[kg\,d^{-1}] = Q_{DSD}\,[m^3\,d^{-1}] \times \rho_{DSD}\,[kg\,m^{-3}]$

Eq (11) $\dot{m}_{15}\,[kg\,d^{-1}] = Q_{15}\,[m^3\,d^{-1}] \times \rho_{15}\,[kg\,m^{-3}]$

To get the mass load rate of 14.centrate ($\dot{m}_{14}$, kg d^{-1}), the mass load rate of 15.biosolids ($\dot{m}_{15}$, kg d^{-1}) was subtracted from mass load rate of DSD ($\dot{m}_{DSD}$, kg d^{-1}):

Eq (12) $\dot{m}_{14}\,[kg\,d^{-1}] = \dot{m}_{DSD}\,[kg\,d^{-1}] - \dot{m}_{15}\,[kg\,d^{-1}]$

The mass load rate of the 14.centrate was converted back to the volume load rate (Q_{14}, $m^3\,d^{-1}$) with the known density of the 14.centrate (ρ_{14}, kg m^{-3}):

Eq (13) $Q_{14}\,[m^3\,d^{-1}] = \dot{m}_{14}\,[kg\,d^{-1}] / \rho_{14}\,[kg\,m^{-3}]$

3.10 Calculation of the daily P mass load rate

The daily P mass load rates ($\dot{m}_{sample\ point}$, kg d^{-1}) were calculated from volume load rates and concentrations of free P ($\gamma(P)_{FP\ sample\ point}$, kg m^{-3}), total P ($\gamma(P)_{TP\ sample\ point}$, kg m^{-3}), and bound P ($\gamma(P)_{BP\ sample\ point}$, kg m^{-3}) per respective sample points as follows:

Eq (14) $\dot{m}_{FP\ sample\ point}\,[kg\,d^{-1}] = Q_{sample\ point}\,[m^3\,d^{-1}] \times \gamma(P)_{FP\ sample\ point}\,[kg\,m^{-3}]$

Eq (15) $\dot{m}_{TP\ sample\ point}\,[kg\,d^{-1}] = Q_{sample\ point}\,[m^3\,d^{-1}] \times \gamma(P)_{TP\ sample\ point}\,[kg\,m^{-3}]$

Eq (16) $\dot{m}_{BP\ sample\ point}\,[kg\,d^{-1}] = Q_{sample\ point}\,[m^3\,d^{-1}] \times \gamma(P)_{BP\ sample\ point}\,[kg\,m^{-3}]$

3.11 Calculation of the anaerobic digester sludge P mass load rate

To calculate the P mass load rates of free P ($\dot{m}_{FP\ 13}$, kg d^{-1}), bound P ($\dot{m}_{BP\ 13}$, kg d^{-1}), and total P ($\dot{m}_{TP\ 13}$, kg d^{-1}) in 13.anaerobic digester sludge, the volume load rate of anaerobic sludge that is pumped to the dewatering step (DSD, digester sludge dewatering $Q_{DSD,}$ $m^3\,d^{-1}$) was used. DSD volume load rate was acquired from the WWTP plant operators:

Eq (17) $\dot{m}_{FP\ 13}$ [kg d^{-1}] = Q_{DSD} [m^3 d^{-1}] x $\gamma(P)_{FP\ 13}$ [kg m^{-3}]

Eq (18) $\dot{m}_{TP\ 13}$ [kg d^{-1}] = Q_{DSD} [m^3 d^{-1}] x $\gamma(P)_{TP\ 13}$ [kg m^{-3}]

Eq (19) $\dot{m}_{BP\ 13}$ [kg d^{-1}] = Q_{DSD} [m^3 d^{-1}] x $\gamma(P)_{BP\ 13}$ [kg m^{-3}]

3.12 Differentiation between biologically and chemically removed P

At the WWTP Eilenburg, P concentration is routinely measured only in the inflow and effluent and removed biologically via bacterial biomass extraction. If a high inflow of P is measured, P is additionally precipitated by adding the chemical precipitant Ferriflock (Kronos International Inc., Leverkusen, Germany). To determine the quantities of both biologically removed P and chemically precipitated P, the total P mass load rate in 1.inflow and in 16.effluent were taken as system boundaries.

3.12.1 Calculation of the total P mass load rate in the 1.inflow

The total P mass load rate of the 1.inflow ($\dot{m}_{TP\ 1}$, kg d^{-1}) was calculated from the volume load rate of 1.inflow (Q_1, m^3 d^{-1}) and total P concentration in the 1.inflow ($\gamma(P)_{TP\ 1}$, kg m^{-3}):

Eq (20) $\dot{m}_{TP\ 1}$ [kg d^{-1}] = Q_1 [m^3 d^{-1}] x $\gamma(P)_{TP\ 1}$ [kg m^{-3}]

3.12.2 Calculation of the total P mass load rate of the 16.effluent

The total P mass load rate of the 16.effluent ($\dot{m}_{TP\ 16}$ kg d^{-1}) was calculated from the volume load rate of 16.effluent (Q_{16}, m^3 d^{-1}) and the total P concentration in the 16.effluent ($\gamma(P)_{TP\ 16}$, kg m^{-3}):

Eq (21) $\dot{m}_{TP\ 16}$ [kg d^{-1}] = Q_{16} [m^3 d^{-1}] x $\gamma(P)_{TP\ 16}$ [kg m^{-3}]

3.12.3 Calculation of the amount of chemically precipitated P

The daily volume load rate of Ferriflock ($Q_{Ferriflock}$, m^3 d^{-1}) was acquired from WWTP operators and the Ferriflock density ($\rho_{Ferriflock}$, kg m^{-3}) from the manufacturer (Kronos International Inc., 2012). The chemical P precipitant Ferriflock has a density ($\rho_{Ferriflock}$) of 1520 kg m^{-3} and contains 123 g iron per kg Ferriflock ($\omega_{Fe\text{-}Ferriflock}$ = 0.123). The mass load rate of added Ferriflock ($\dot{m}_{Ferrifloc}$, kg d^{-1}) was calculated from Ferriflock volume load rate ($Q_{Ferrifloc}$ m^3 d^{-1}) and Ferriflock density ($\rho_{Ferriflock,}$, kg m^{-3}):

Eq (22) $\dot{m}_{Ferriflock}$ [kg d^{-1}] = $Q_{Ferriflock}$[m^3 d^{-1}] x $\rho_{Ferriflock}$ [kg m^{-3}]

The mass load rate of iron (Fe ion) in Ferriflock ($\dot{m}_{Fe}$, kg d^{-1}) was calculated from known mass load rate of added Ferriflock ($\dot{m}_{Ferriflock}$, kg d^{-1}) and iron mass content in the Ferriflock ($\omega_{Fe\text{-}Ferriflock}$):

Eq (23) $\dot{m}_{Fe}$ [kg d^{-1}] = $\dot{m}_{Ferrifloc}$ [kg d^{-1}] * $\omega_{Fe\text{-}Ferriflock}$

The Fe ion dosage of Ferriflock is 1.5 Fe ions for every elementary P (WWTP operator, personal communication 2019). The molar ratio of Fe to P is 2.7, which means that 2.7 kg of Ferriflock precipitates 1 kg of P under the assumption that each Fe ion is used without by-product formation. Therefore, precipitated P mass load rate ($\dot{m}_{Pprecip}$, kg d^{-1}) can be calculated as follows:

Eq (24) $\dot{m}_{Pprecip}$ [kg d^{-1}] = $\dot{m}_{Fe}$ [kg d^{-1}] / 2.7

3.12.4 Calculation of the amount of biologically removed P

The P mass load rate of biologically removed P ($\dot{m}_{Pbiol}$, kg d^{-1}) was calculated by subtracting the total P mass load rate precipitated ($\dot{m}_{Pprecip}$, kg d^{-1}) and the total P mass load rate in the 16.effluent ($\dot{m}_{TP\ 16}$, kg d^{-1}) from total P mass load rate of 1.inflow ($\dot{m}_{TP\ 1}$, kg d^{-1}):

Eq (25) $\dot{m}_{Pbiol}$ [kg d^{-1}] = $\dot{m}_{TP\ 1}$ [kg d^{-1}] - $\dot{m}_{Pprecip}$ [kg d^{-1}] - $\dot{m}_{TP\ 16}$ [kg d^{-1}]

3.12.5 Calculation of the WWTP P removal efficiency

To calculate the WWTP P removal efficiency the total P mass load rate of the 1.inflow ($\dot{m}_{TP\ 1}$, kg d^{-1}) and of the 16.effluent ($\dot{m}_{TP\ 16}$, kg d^{-1}) must be known. The total P mass load rate of the 1.inflow and the 16.effluent was calculated as shown in Eq 20 and 21.

With total P mass load rate of the 1.inflow and that of the 16.effluent known, the removal efficiency (RE, %) was calculated:

Eq (26) RE [%] = 100 [%] – (($\dot{m}_{TP\ 16}$ [kg d^{-1}] / $\dot{m}_{TP\ 1}$ [kg d^{-1}]) x 100 [%])

All values and results of the calculations are shown in SI Table 3.

4 RESULTS

4.1 P concentrations in process streams

P should be removed from WWTP process streams and made available to the market at certain levels of P concentrations. In this study, the critical level of P concentration was set to 20 g P kg_{DM}^{-1} (AbfKlärV, 2017) and to 0.05 kg m^{-3} free P and bound P according to Cornel and Schaum (2009), who first established this limit for feasibility of P recovery. Economically inefficient process streams were: 1.inflow, 2.grit chamber start, 3.grit chamber end, 4.primary clarifier, 9 and 10.secondary clarifier1,2 and 16.effluent. These process streams do not reach either of the two critical levels required (Figure 2, lower left quarter of the graph) to make P recovery economical. Process streams, where free P concentrations and bound P

concentrations together were above the defined economically feasible P concentration threshold were: 5.primary sludge, 6. and 7.aeration tank1,2, 11.return sludge, 12.excess sludge, 13.anaerobic digester sludge, 14.centrate and 15.biosolids. Therefore, these process streams seem to be suitable as a means to reduce P concentrations in the liquid and solid phases. Both phases contain bound P and free P in different proportions. In comparison to bound P, free P is the economically more interesting component.

The following process streams were found to contain even free P concentrations above a threshold of 0.05 kg m^{-3}: 5.primary sludge, 13.anaerobic digester sludge, 14.centrate and water-extracts of 15.biosolids with 0.131 kg m^{-3}, 0.510 kg m^{-3}, 0.075 kg m^{-3} and 1.023 kg m^{-3}, respectively. The daily P mass load rate of free P was 7.279 kg d^{-1}, 38.226 kg d^{-1}, 4.820 kg d^{-1} and 9.919 kg d^{-1}, respectively (SI Table 7). All four sources of high free P quantities are represented in the upper part of Figure 2. Process stream 5.primary sludge should not be used for P recovery due to significant health implications of the still nearly untreated wastewater constituents. Therefore, the most obvious locations for free P recovery would be 13.anaerobic digester sludge, 14.centrate and 15.biosolids (water-extracts).

Bound P consists of biomass bound P and chemically precipitated P. Bound P concentrations were above an economically feasible level of 0.05 kg m^{-3} in process streams 5.primary sludge, 6. and 7.aeration tank1,2, 11.return sludge, 12.exces sludge, 13.anaerobic digester sludge, and 15.biosolids. Here too, 5.primary sludge was excluded from P recovery strategies for hygienic reasons. Also, the most active part of the wastewater purification system 6. and 7.aeration tank1,2 should not be part of a P-recovery solution in order not to impair its active wastewater treatment function. Thus, the process streams with high bound P load were 11 - 13 and the solids of 15 with bound P concentrations of 0.300 kg m^{-3}, 0.268 kg m^{-3}, 0.213 kg m^{-3}, and 1.336 kg m^{-3}, respectively, and daily bound P mass load rates of 1147.548 kg d^{-1}, 31.880kg d^{-1}, 17.180 kg d^{-1} and 13.156 kg d^{-1}, respectively (SI Table 7). The four process streams are visualized in the upper part of Figure 2. The highest concentration of bound P was found in the solids of 15.biosolids. The shares of bound P within total P in 13.anaerobic digester sludge and 15.biosolids were 29.5 % and 57.01 % (Figure 2, SI Table 7). Bound P from 11.return sludge was returned to the 6. and 7.aeration tanks1,2 and, if P is not recovered, the P content in these process streams is always similar to 11.return sludge. The amounts of bound P in these streams reached 80-96 % of the total P (Figure 2). Ultimately, the most promising stages for the recovery of bound P are 11.return sludge and somewhat less, due to the lower bound P mass load rate, the 12.excess sludge as well as the 13.anaerobic digester sludge and the solids of the 15.biosolids.

The P content in DM of process streams leaving the WWTP should be below the limit of 20 g P kg_{DM}^{-1}, otherwise P must be mandatory recovered by any available P recovery technology (AbfKlärV, 2017). In the

following process streams the P content in DM was above this limit: 6. and 7.aeration tank1-2, 11.return sludge, 12.excess sludge and 15. biosolids with 24.843g P kg_{DM}^{-1}, 25.671g P kg_{DM}^{-1}, 32.591g P kg_{DM}^{-1}, 26.519 g P kg_{DM}^{-1}, and 24.420 g P kg_{DM}^{-1}. With exception of the final waste stream 15.biosolids, none of these process streams are subject to the legal limit. Nevertheless, these numbers also indicate that 11.return sludge and 12.excess sludge are valuable sources for the recovery of bound P. Figure 2 highlights 11.return sludge and 12.excess sludge in the right part of Figure 2, far from the vertical red line marking the legally allowed amount of 20 g P kg_{DM}^{-1}.

Furthermore, in 16.effluent the P content in DM was high with 18.040g P kg_{DM}^{-1}. Due to the low amount of biomass in 16.effluent, the daily mass load rate of bound P was 1.645 kg d^{-1} within the total P concentration of 0.0011 kg m^{-3}.

4.2 P removal efficiency

The WWTP P removal efficiency RE is described as difference between the total P concentrations of 16.effluent and 1.inflow (Eq 26). The P removal average amount per day was 89.21 % (± 6.2 %, SI Table 3). SI Figure 3 shows a graphical representation on the mass load of total P ($\dot{m}$TP [kg day^{-1}]) arriving at the WWTP and how much of it is biologically removed or chemically precipitated and how much of it is lost via the 16.effluent. The removal efficiency can be derived from the $\dot{m}$TP against the loss of P via 16.effluent. The variation of the observed values of the $\dot{m}$TP results from the differing daily volume load rates and total P concentration of the 1.inflow, while the P loss of the 16.effluent is determined by the daily P removal either chemically and biologically.

4.3 Proportions of biologically removed and chemically precipitated P

In this study, P was frequently chemically precipitated with iron salts at the sampling point 8.precipitation shaft. Chemically precipitated P cannot easily be used for biological P recovery strategies. To know the effect of the chemical precipitation on biological P removal, the different proportions of chemically precipitated and biologically bound P were calculated by subtracting the $\dot{m}$TP precipitated by Ferrifloc (12.45 kg d^{-1}, ±7.74) and the $\dot{m}$TP lost via the effluent (4.47 kg d^{-1}, ±2.14) from $\dot{m}$TP entering the WWTP (43.15 kg d^{-1}, ±10.55), thereby gaining the $\dot{m}$TP, which is biologically removed (27.05 kg d^{-1}, ±11.51) (SI Figure 3, SI Table 3). The SI Figure 3B, C shows the $\dot{m}$TP for either chemically precipitated P or biologically removed P, which are later used to distinguish days with rather biological removal from days with rather chemical precipitation in order to infer the role of precipitation in biological removal. Complete calculation

steps for the determination of amounts of precipitated P vs. biologically bound P were provided (Eq 20 – Eq 25).

4.4 The composition of the microbial communities in the process streams

To describe the different capacities of the microorganisms to bind P in the different process streams, the structures of the microbial community were analyzed by flow cytometry (exemplary cytometric data are shown in SI Figure 4 and the whole data set as a video in SI video 1). Cell abundance calculations per subcommunity are visualized in NMDS-plots for each of these microbial communities (Figure 3), visualizing similarities between communities per process stream for all sampling days based on Bray-Curtis dissimilarity measure. Each circle in Figure 3 represents a community and the size of the circles corresponds to the time sequence of sampling per sampling point. The similarity between microbial communities per sampling point is the higher, the closer the circles are to each other, and the closer the circles are to the NMDS-plot centroid (black cross in the respective plots). Differences between the microbial communities are observed both by the spread of the circles and by their distance changes from the centroid of an NMDS-plot (centroids and average distances are given in SI Table 5). In general, it was found that the microbial community structures were different between all 16 process streams although similar process steps also showed similar microbial community structures such as 1.inflow to 4.primary clarifier or 6. and 7.aeration tanks1,2 and 12.return sludge. But the variation within the communities of each of the individual process streams was often small and only the communities in 9. and 10.secondary clarifier1,2, 14.centrate and 16.effluent changed their structure over time (Figure 3).

4.5 The functional relationship between microbial communities and free P and bound P values

As P accumulation is a universal trait in microorganisms it can be expected that many of them are capable of binding P in high quantities. In the following analyses, only process streams with bound and free P concentrations above economically feasible concentrations for P recovery were included (process streams in the upper part of Figure 2). Furthermore, microbial community data, obtained by flow cytometry and evaluated using the tool flowCyBar, were included in the analysis. As shown in Figure 3, no major dynamics in the community structures were found for the relevant process streams. To investigate the depth of interaction of the microbial communities with bound P and free P a correlation analysis using Spearmans ranked order correlation coefficient rho was performed. The correlations were done in iterative steps adding a further sampling day in each step for each process stream until the end of the sampling campaign. Correlations between P types with SCs with a significance value $P<0.05$ were counted per process stream

and day and the sum of all correlations per process stream was corrected by the number of days and the number of involved SCs (SCs = nr.gates). Only those SCs were included that showed an average cell abundance above 1%. The resulting values are given as ∑ corr. d^{-1} $nr.gates^{-1}$. An overview of all obtained data is given in form of heatmaps in SI Figure 5. A circos plot (Gu et al., 2014) was used to visualize the corrected number of correlations between microbial communities and bound P and free P concentrations (Figure 4).

We found strong positive correlations between bound P and the microbial communities of all process streams, indicating a high capacity of cells to accumulate P both by cell growth and by storage of P as poly-P. For P accumulation they need to feed on free P. Negative correlations between microorganisms and free P concentrations reflect this episode. All process streams except 5.primary sludge show negative correlations within this context. The sum of the number of positive correlations with bound P was $n_{corr.}$=0.17 ∑ corr. d^{-1} $nr.gates^{-1}$, while that of negative correlations with free P was $n_{corr.}$=0.45 ∑ corr. d^{-1} $nr.gates^{-1}$ (Figure 4). Negative correlations of cell abundances to bound P values were also observed for all process streams except 5.primary sludge and are expected to indicate organisms that have not contributed to P accumulation. This is to be expected since not all organisms can be assumed to have the ability to store P or grow during wastewater treatment. Strong positive correlations between microorganisms and free P indicate release of P, e.g. by anaerobic conditions. The number of negative correlations with bound P ($n_{corr.}$=0.31 ∑ corr. d^{-1} $nr.gates^{-1}$) was higher than the positive ones, while positive correlations to free P, which coincided with P release, were lower ($n_{corr.}$=0.17 ∑ corr. d^{-1} $nr.gates^{-1}$, Figure 4). The last two types of correlations were found in all sampling points except 5.primary sludge were only positive correlations were found. As a result, we can state that the capacity for biological accumulation of P was high in all relevant process streams, but an almost equal number of correlations indicated also organisms that were not strongly involved in this function.

4.6 The influence of chemical P precipitation on the P accumulation capacity of microorganisms

How chemical precipitation might impact the ability of the cells to bind P was investigated by determining the number of functional interactions of microbial SCs with chemically precipitated or biologically bound P and the amount of free P using the strong correlations (P<0.05). Again, only process streams with bound and free P concentrations above economically feasible concentrations for P recovery were included into the analyses as well as the 8.precipitation shaft, where the precipitant was added. To achieve a separation of days with high biological P removal and those with high chemical P precipitation, the days fitting into the upper 25 % quintile (8 days with highest P removed biologically > 36.28 kg d^{-1}, 8 days with highest P

chemically precipitated > 15.65 kg d^{-1}, SI Figure 3) were used for the correlation analysis, respectively. An overview of the correlation and corresponding P values is given in form of heatmaps in SI Figure 6. On days with rather biological P removal, an average of 42.69 kg d^{-1} P was biologically removed P compared to 9.46 kg d^{-1} chemically precipitated P, the amounts of which were reversed on days with rather chemical P precipitation with 16.99 kg P d^{-1} compared to 23.64 kg P d^{-1}.

On days with rather biological P removal, high numbers of positive correlations to biologically bound P ($n_{poscorrBP.}$=0.09 ∑ corr. d^{-1} $nr.gates^{-1}$) were found (Figure 5). The number of negative correlations with free P was also high ($n_{negcorrFP}$= 0.24 ∑ corr. d^{-1} $nr.gates^{-1}$). All process streams showed a capacity to bind P biologically and the ability to take up free P (except 13.anaerobic digester sludge, Figure 5, right side), similar to the P removal capacity shown in Figure 4.

Chemical treatment led to a decreased number of positive correlations with biological bound P ($n_{poscorrBP}$= 0.05 ∑ corr. d^{-1} $nr.gates^{-1}$) and an equally lower number of negative correlations with free P ($n_{negcorrFP}$= 0.15 ∑ corr. d^{-1} $nr.gates^{-1}$; Figure 5, left side). In 11.return sludge no evidence for biological P removal could be found in contrast to the days with rather biological P removal. Obviously, the chemical precipitation of P seems to negatively impact the availability of free P and to cause a decreased ability of microorganisms to accumulate P biologically.

5 DISCUSSION

5.1 The framework for P-cycle assessment

P can be recovered from both the liquid and solid phases of the process streams and potential operators of P recovery plants can choose from a wide range of technologies (Schönberg et al., 2018; Egle et al., 2016; 2015; Petzet and Cornel, 2013). Updated lists of full-scale recovery plants can be found on the ESPP platform (https://www.phosphorusplatform.eu/activities/p-recovery-technology-inventory), or in (Kabbe et al., 2017; Walker, 2017). Newly emerging P bio-based recovery technologies, which are mostly still on research or pilot stages with a few demonstration plants, are summarized in Carrillo et al., 2020; Roy, 2017 and Tarayre et al., 2016. However, bio-based P recovery technologies that can be applied on-site at a full-scale WWTP and in-time of the ongoing operation of wastewater treatment are not yet available.

This study helps to prevent the loss of anthropogenic P by providing a framework for P-cycle assessment in typical full-scale WWTPs to mark the process stages where P can be immediately recovered on-site. The legally permitted 20 g P kg_{DM}^{-1} (AbfKlärV, 2017) and the 0.05 kg P m^{-3} (Cornel and Schaum, 2009) were set

as thresholds both for free P and bound P as well as for the respective P types. In a first step, the study relied on a common basis of generated P-data with total P, bound P and free P as the only P types. In a second step, a framework for P-cycle assessment was established, which is universal, even though there may be different technological levels and operational backgrounds between WWTPs. Currently, there is no consensus on a uniform calculation basis for P types in different process streams of a WWTP. In this study generally available and EU ISO standards were used, which ensures repeatability and comparability of the data. All values were calculated using the developed framework for P-cycle assessment and allow decisions to be made on process streams feasible for (biological) P recovery as well as for the reduction of P in liquid and solid phases.

In the example full-scale WWTP investigated in the study, feasible options for the P recovery of bound P in the sludge were process streams 11.return sludge, 12.excess sludge, 13.anaerobic digester sludge, and 15. biosolids. Both the 11.return sludge and the 12.excess sludge had a P content in DM above the legally permissible values with similar values as they are coming from the same source, but their daily P mass load rates were quite different with a proportion of about 26 : 1. In these two process streams the bound P usually remains in a WWTP unless it is recovered by special in-stream technologies, which would be an option to keep the over-all P content low in a WWTP. The in-stream treatment of the 13.anaerobic digester sludge is also a possibility to reduce its P content, as otherwise the 14.centrate as a successive process stream returns the P back into the 6. and 7.aeration tanks1,2. This is different for the bound P in 15.biosolids, which is a waste stream that leaves the WWTP and can be straightforwardly handled for biological P removal at the end of the process.

Feasible options for free P recovery were 13.anaerobic digester sludge, 14.centrate and 15.biosolids. The best biological P recovery approach for free P would be the use of the liquid phases. For 13.anaerobic digester sludge and 14.centrate there are already technological-scale solutions available but only for applications connected to chemical precipitation (Schönberg et al., 2018; Egle et al., 2016). For 15.biosolids an enormous release of free P after treatment with water with up to 1.023 kg m^{-3} was found. The high extractability of free P from biosolids with water has already been described (Torri et al., 2017) and seems to be a promising and practicable solution for biological P recovery. 15.biosolids would therefore be a good source for recovery of free P if they are first dissolved in water before disposed of, e.g. by mono-incineration. Thus, in the example full-scale WWTP promising process streams were identified from which free or bound P could be recovered in large quantities. This would not only help to meet the legally prescribed limits for P concentrations in waste streams, but also to prevent struvite

formation in pipes and anaerobic digesters, where high P concentrations have been shown to reduce the methane production (Günther et al., 2016).

5.2 P accumulation by microbial communities

Active microbial communities are at the functional basis of a WWTP. Arriving with the incoming wastewater they build up distinct communities with water cleaning capabilities (Ali et al., 2019; Saunders et al., 2016). Flow cytometry is a highly suitable method to study the dynamics in composition of immanent microbial communities (Haange et al., 2020; Liu et al., 2019; Liu et al., 2018; Koch et al., 2014) and this method was also used in this study to link WWTP microbial community dynamics to P distribution. Significant differences in the composition of the communities between different process stages were already described (Numberger et al., 2019; Zhang et al., 2019; Günther et al., 2016; Wells et al., 2014) and similar results were obtained in this study. The process streams 1 to 5 (1.inflow to 5.primary sludge) belong to the stage of mechanical wastewater treatment and proved to be very similar. The process streams of biological wastewater treatment with process streams 6 - 8 and 11, 12, 15 were also similar in structure and even showed no intermittent fluctuations in the composition over the two years of sampling. Process stages with low cell density and low nutrient content (process streams 9, 10, and 16) differed significantly from the other process stages and showed strongly fluctuating patterns over the period studied. It can be assumed that concrete weather events (Isazadeh et al., 2016; Otterpohl and Freund, 1992) and temperature (Numberger et al., 2019; Tejaswini et al., 2019) could have had a greater impact on these community structures compared to the preceding streams. The community compositions of 13.anaerobic digester sludge and the 14.centrate differed in their structure from all others, which can be attributed to the need for different functionality of these two process stages, as demonstrated earlier (Günther et al., 2016). A relatively constant community composition was also shown at the phylum level by de Celis et al. (2020) and Zhang et al. (2018), where selected streams or different types of activated sludge were analyzed up to a period of two years. Similar to our findings, they found a higher community dispersion only in stages with low biomass contents such as the liquid fractions of the secondary clarifiers, the centrate and the effluent. In general, however, it can be assumed that core communities are found in most communities. Wu et al. (2019) recently described the global core community of activated sludge, which comprises 28 OTUs. We found 13 to 26 constant SCs in the (activated) sludge stages (SI Table 8), which is comparable to these results.

The uptake of free P into the biomass is either by growth (Zhao and Liu, 2013) or by poly-P accumulation (Feng et al., 2020). Instead, P is released by cell degradation (Sharma et al., 2013) or by release of free P

under anaerobic conditions, as in anaerobic digestion or in the anaerobic stages of activated sludge treatment and all stages containing sludge (Feng et al., 2020; Yang et al., 2017). The high correlation numbers between the free and bound P fractions in all process streams with sludge fractions and even for 14.centrate suggested the uptake of free P and its binding into the biomass (Figure 4). The same correlation pattern was also found in the 13.anaerobic digester sludge, although here the P binding occurs under anaerobic conditions. Denitrificating phosphate accumulating organisms from 11.return sludge, such as species belonging to the *Proteobacteria* like *Candidatus Accumulibacter phosphatis*, could be responsible for this (Mukherjee et al., 2019; Yang et al., 2017; Günther et al., 2012). It has also been shown that archaea of the genera *Methanosarcina*, *Methanoregula*, *Methanolobus* accumulate polyphosphates (Paula et al., 2019). Members of the genus *Methanosarcina* were found to be present in the investigated digester (Günther et al., 2016).

5.3 The influence of chemical P precipitation on the P accumulation capacity of microorganisms

As the results have shown, high P concentrations are to be expected in most of the process streams. High P concentrations in the sludge are likely to lead to struvite formation in the pipes and digesters, which may affect maintenance costs and operation (Kehrein et al., 2020; Günther et al., 2016; Fattah et al., 2008). Therefore, chemical P precipitation is an efficient back-fall solution in WWTPs if the P concentrations in the process streams are too high. Nevertheless, biologically P removal is most often preferred because the costs are reduced if chemical precipitation of P can be dispensed with (Cramer et al., 2018; Paul et al., 2001). In addition, P precipitated by metals cannot be easily recovered and would require forceful chemical P desorption technologies (Bashar et al., 2018; Wilfert et al., 2015). For the WWTP Eilenburg, chemical P removal was performed frequently, indicating that there is room for improvement in biological P recovery, yet the discharge of P into the environment was always below the legal maximum limit.

The correlation analyses revealed that the biological P removal functions between days with rather biological P removal were different compared to days with rather chemical P precipitation at the WWTP Eilenburg (Figure 5). Although P accumulating bacteria inhibiting concentrations of iron (40 g m^{-3}, Yilmaz et al., 2017) were not reached, the adverse effect of limited availability of free P, which affects the biological capacity to form bound P appears to be reduced. In a P recovery technology based on biological P removal, high concentrations of chemically precipitated P can have serious consequences for recovery efficiency, as chemically precipitated P amasses and cannot be taken up directly by microorganisms. The biological uptake of P is a fast process, but chemical precipitation is much faster and P is therefore lost to

631 microorganisms as soon as precipitants are added (de Haas et al. 2001). Experiments with ferric chloride
632 have shown that lower amounts of iron (10-20 g m^{-3}) lead to a competition between biological P uptake
633 and P precipitation if the available amount of free P is small (Liu et al., 2011; de Haas et al., 2001).
634 However, the fact that biological P removal indicators are still found on days with rather chemical
635 precipitation shows that there is no permanent impact on the microbial P removal activity.
636
637 **6 CONCLUSION**
638 A framework for P-cycle assessment in WWTPs was developed on the basis of standardized P types and P
639 type analyses methods. An example full-scale WWTP was studied and a unified approach for P
640 concentration assessment was run to calculate P mass load rates for 16 process streams for about two
641 years. Using the framework for P-cycle assessment, we were able to identify WWTP process streams that
642 can be used for biological P recovery from an economic point of view, making it easier in future to comply
643 with legal regulations on P contents. In addition, we gained insight into the dependencies of the microbial
644 communities to the antagonistic impacts of chemical precipitation on biological P accumulation in the
645 different process streams.
646 The framework for P-cycle assessment can lead to large amounts of unified data gathered from WWTP
647 process streams in further studies and will facilitate decisions on application of recovery strategies. Based
648 on knowledge of the distribution of free and bound P between process streams new in-stream P recovery
649 strategies can be designed, preferably on-site and in-time, that fit to the individual design of a WWTP
650 without disrupting the functioning of the wastewater purification and at the same time avoiding the loss
651 of a non-renewable resource.
652
653 **ACKNOWLEDGMENTS**
654 We thank the operators of the WWTP Eilenburg for help with the sampling and supplying technical
655 information, and the Abwasserzweckverband Mittlere Mulde for the access to the WWTP as well as
656 supplication of the operational data sets.
657
658 **FUNDING**
659 This work was supported by the Deutsche Bundesstiftung Umwelt DBU [grant number 33960/01-32] and
660 the Bundesministerium für Wirtschaft und Energie [grant number 16KN043226].
661
662 **AUTHOR CONTRIBUTIONS**

VV: conceptualization, methodology, framework of P-cycle assessment, calculation and evaluation of data, validation of data, writing; CS: sampling, methodology, flow cytometry; HH: reviewing, editing; SM: conceptualization, writing, reviewing, editing; SG: data curation, visualization, reviewing, editing.

DECLARATION OF INTEREST

The authors have no competing interests to declare.

REFERENCES

AbfKlärV, 2017. Verordnung zur Neuordnung der Klärschlammverwertung, in: Bundesministerium für Umwelt NunSB, editor. Bundesgesetzblatt Jahrgang 2017 Bundesgesetzblatt Jahrgang 2017 Teil I Nr 65. Bundesministerium für Umwelt, Naturschutz und nukleare Sicherheit (BMU), Bonn, Germany.

AbwV, 2020. 17. Juni 2004 (BGBl. I S. 1108, 2625), 6. März 2020 (BGBl. I S. 485), Bonn, Germany.

Ahn, J., Schroeder. S., Beer, M., McIlroy, S., Bayly, R.C., May, J.W., Vasiliadis, G., Seviour R.J., 2007. Ecology of the Microbial Community Removing Phosphate from Wastewater Under Continuously Aerobic Conditions in a Sequencing Batch Reactor. Appl. Environ. Microbiol., 73, 2257-2270. https://doi.org/10.1128/AEM.02080-06

Ali, M., Wang, Z., Salam, K.W., Hari, AR., Pronk, M., van Loosdrecht, M.C.M., Saikaly, P.E., 2019. Importance of Species Sorting and Immigration on the Bacterial Assembly of Different-Sized Aggregates in a Full-Scale Aerobic Granular Sludge Plant. Environ. Sci. Technol., 53, 8291-8301. https://doi.org/10.1021/acs.est.8b07303

Bashar, R., Gungor, K., Karthikeyan, K.G., Barak, P., 2018. Cost Effectiveness of Phosphorus Removal Processes in Municipal Wastewater Treatment. Chemosphere, 197, 280-290. https://doi.org/10.1016/j.chemosphere.2017.12.169

Blackall, L., Crocetti, G., Saunders, A., Bond, P., 2002. A Review and Update of the Microbiology of Enhanced Biological Phosphorus Removal in Wastewater Treatment Plants. Antonie van Leeuwenhoek, 81, 681-91. https://doi.org/10.1023/A:1020538429009

Car, D., Lewin-Koh, N., Maechler, M., Sarkar, D., 2019. Hexbin: Hexagonal Binning Routines. R package version 1.27.2.

Carrillo, V., Fuentes, B., Gómez, G., Vidal, G., 2020. Characterization and Recovery of Phosphorus from Wastewater by Combined Technologies. Rev. Environ. Sci. Biotechnol., 19, 389-418. https://doi.org/10.1007/s11157-020-09533-1

Cichocki, N., Hübschmann, T., Schattenberg, F., Kerckhof, F.M., Overmann, J., Müller, S., 2020. Bacterial Mock Communities as Standards for Reproducible Cytometric Microbiome Analysis. Nat. Protoc. DOI: 10.1038/s41596-020-0362-0, on-line

697 Cieślik, B., Konieczka, P., 2017. A Review of Phosphorus Recovery Methods at Various Steps of Wastewater
698 Treatment and Sewage Sludge Management. The Concept of “No Solid Waste Generation” and Analytical
699 Methods. J. Clean. Prod., 142, 1728-1740. https://doi.org/10.1016/j.jclepro.2016.11.116

700 COM., 2017. Communication from the Commission to the European Parliament, the Council, the European
701 Economic and Social Committee and the Committee of the Regions on the 2017 list of Critical Raw
702 Materials for the EU. COM (2017) 490 final. Eurpean Commission, Brussels, pp. 14.

703 Cordell, D., Drangert, J.O., White, S., 2009. The Story of Phosphorus: Global Food Security and Food for
704 Thought. Glob. Environ. Change., 19, 292-305. https://doi.org/10.1016/j.gloenvcha.2008.10.009

705 Cornel, P., Schaum, C., 2009. Phosphorus Recovery from Wastewater: Needs, Technologies and Costs.
706 Water Sci. Technol., 59, 1069-76. https://doi.org/10.2166/wst.2009.045

707 Cramer, M., Koegst, T., Traenckner, J., 2018. Multi-criterial Evaluation of P-Removal Optimization in Rural
708 Wastewater Treatment Plants for a Sub-Catchment of the Baltic Sea. Ambio, 47, 93-102.
709 https://doi.org/10.1007/s13280-017-0977-8

710 Daneshgar, S., Callegari, A., Capodaglio, A., Vaccari, D., 2018. The Potential Phosphorus Crisis: Resource
711 Conservation and Possible Escape Technologies: A Review. Resources, 7(2), 37.
712 https://doi.org/10.3390/resources7020037

713 de Celis, M., Belda, I., Ortiz-Álvarez, R., Arregui, L., Marquina, D., Serrano, S., Santos, A., 2020. Tuning Up
714 Microbiome Analysis to Monitor WWTPs’ Biological Reactors Functioning. Sci. Rep., 10, 4079.
715 https://doi.org/10.1038/s41598-020-61092-1

716 de Haas, D.W., Wentzel, M.C., Ekama, G.A., 2001. The Use of Simultaneous Chemical Precipitation in
717 Modified Activated Sludge Systems Exhibiting Biological Excess Phosphate Removal Part 5: Experimental
718 Periods Using a Ferrous-ferric Chloride Blend. Water SA, 27(2), 117-134. DOI: 10.4314/wsa.v27i2.4987

719 de Haas, D.W, Wentzel, M.C., Ekama, G.A, 2001. The Use of Simultaneous Chemical Precipitation in
720 Modified Activated Sludge Systems Exhibiting Biological Excess Phosphate Removal Part 6: Modelling of
721 Simultaneous Chemical-Biological P Removal - Review of Existing Models. Water SA, 27(2), 135-150. DOI:
722 10.4314/wsa.v27i2.4988

723 Desmidt, E., Ghyselbrecht, K., Zhang, Y., Pinoy, L., der Bruggen, B.V., Verstraete, W., Rabaey, K.,
724 Meesschaert, B., 2015. Global Phosphorus Scarcity and Full Scale P Recovery Techniques: A Review. Crit.
725 Rev. Environ. Sci. Technol., 45, 336-384. https://doi.org/10.1080/10643389.2013.866531

726 DIN EN ISO 6878:2004-09., 2004. Water quality - Determination of Phosphorus - Ammonium Molybdate
727 Spectrometric Method

728 DIN EN ISO 17294-2:2017-01., 2017. Water quality - Application of Inductively Coupled Plasma Mass
729 Spectrometry (ICP-MS) - Part 2: Determination of selected elements including uranium isotopes.

730 Egle, L., Rechberger, H., Krampe, J., Zessner, M., 2016. Phosphorus Recovery from Municipal Wastewater:
731 An Integrated Comparative Technological, Environmental and Economic Assessment of P Recovery
732 Technologies. Sci. Total. Environ., 571, 522-542. https://doi.org/10.1016/j.scitotenv.2016.07.019

733 Egle, L., Rechberger, H., Zessner, M., 2015. Overview and Description of Technologies for Recovering
734 Phosphorus from Municipal Wastewater. Resour. Conserv. Recycl., 105, 325-346.
735 https://doi.org/10.1016/j.resconrec.2015.09.016

736 Fattah, K.P., Sabrina, N., Mavinic, D.S., Koch, F.A., 2008. Reducing Operating Costs for Struvite Formation
737 With a Carbon Dioxide Stripper. Water Sci. Technol., 58(4), 957-962.
738 https://doi.org/10.2166/wst.2008.722

739 Feng, C., Welles, L., Zhang, X., Pronk, M., de Graaff, D., van Loosdrecht, M., 2020. Stress-induced Assays
740 for Polyphosphate Quantification by Uncoupling Acetic Acid Uptake and Anaerobic Phosphorus Release.
741 Water Res., 169, 115228. https://doi.org/10.1016/j.watres.2019.115228

742 Gu, Z., Gu, L., Eils, R., Schlesner, M., Brors, B., 2014. Circlize Implements and Enhances Circular
743 Visualization in R. Bioinformatics, 30, 2811-2. https://doi.org/10.1093/bioinformatics/btu393

744 Günther, S., Faust, K., Schumann, J., Harms, H., Raes, J., Muller, S., 2016. Species-Sorting and Mass-
745 Transfer Paradigms Control Managed Natural Metacommunities. Environ. Microbiol., 18, 4862-4877.
746 https://doi.org/10.1111/1462-2920.13402

747 Günther, S., Grunert, M., Müller, S., 2018. Overview of Recent Advances in Phosphorus Recovery for
748 Fertilizer Production. Eng. Life Sci., 18. https://doi.org/10.1002/elsc.201700171

749 Günther, S., Koch, C., Hübschmann, T., Röske, I., Müller, R.A., Bley, T., Harms, H., Müller, S., 2012.
750 Correlation of Community Dynamics and Process Parameters as a Tool for the Prediction of the Stability
751 of Wastewater Treatment. Environ. Sci. Technol., 46(1), 84-92. https://doi.org/10.1021/es2010682

752 Haange, S.B., Jehmlich, N., Krügel, U., Hintschich, C., Wehrmann, D., Hankir, M., Seyfried, F., Froment, J.,
753 Hübschmann, T., Müller, S., Wissenbach, D.K., Kang, K., Buettner, C., Panagiotou, G., Noll, M., Rolle-
754 Kampczyk, U., Fenske, W., von Bergen, M., 2020. Gastric Bypass Surgery in a Rat Model Alters the
755 Community Structure and Functional Composition of the Intestinal Microbiota Independently of Weight
756 Loss. Microbiome, 8, 13. https://doi.org/10.1186/s40168-020-0788-1

757 Hahne, F., LeMeur, N., Brinkman, R.R., Ellis, B., Haaland, P., Sarkar, D., Spidlen, J., Strain, E., Gentleman,
758 R., 2009. flowCore: a Bioconductor Package for High Throughput Flow Cytometry. R Package Version
759 1.52.1. BMC Bioinformatics, 10, 106. https://doi.org/10.1186/1471-2105-10-106

760 Harrell, F.E., Dupont, C. et al. ., 2018. Hmisc: Harrell Miscellaneous. R package version 4.1-1.Hijmans, R.,
761 van Etten, J., 2014. Raster: Geographic Data Analysis and Modeling. R package version 3.0-7. R Package
762 Version 2014; 517, 2-12.

763 Isazadeh, S., Jauffur, S., Frigon, D., 2016. Bacterial Community Assembly in Activated Sludge: Mapping
764 Beta Diversity Across Environmental Variables. Microbiologyopen, 5, 1050-1060.
765 https://doi.org/10.1002/mbo3.388

766 Kabbe, C., Kraus, F., 2017. P Recovery: From Evolution to Revolution. Fertilizer International, 479, 37–41.

767 Kehrein, P., van Loosdrecht, M., Osseweijer, P., Garfí, M., Dewulf, J., Posada, J., 2020. A Critical Review of
768 Resource Recovery from Municipal Wastewater Treatment Plants – Market Supply Potentials,

769 Technologies and Bottlenecks. Environ. Sci.: Water Res. Technol., 6, 877-910.
770 https://doi.org/10.1039/C9EW00905A

771 Kronos International Inc., 2012. Phosphateliminierung mit Eisensalzen. Leverkusen, p.p. 7.
772 https://kronosecochem.com/wp-content/uploads/TI_3_01_DE_Phosphateliminierung.pdf (accessed
773 19.07.2020).

774 Koch, C., Fetzer, I., Schmidt, T., Harms, H., Müller, S., 2013. Monitoring Functions in Managed Microbial
775 Systems by Cytometric Bar Coding. Environ. Sci. Technol., 47, 1753-1760.
776 https://doi.org/10.1021/es3041048

777 Koch, C., Harms, H., Müller, S., 2014. Dynamics in the Microbial Cytome—Single Cell Analytics in Natural
778 Systems. Curr. Opin. Biotechnol., 27, 134-141. https://doi.org/10.1016/j.copbio.2014.01.011

779 Kok, D.J.D., Pande, S., van Lier, J.B., Ortigara, A.R.C., Savenije, H., Uhlenbrook, S., 2018. Global Phosphorus
780 Recovery from Wastewater for Agricultural Reuse. Hydrol. Earth Syst. Sci., 22, 5781-5799.
781 https://doi.org/10.5194/hess-2018-176

782 Law, K., Pagilla, K., 2018. Phosphorus Recovery by Methods Beyond Struvite Precipitation. Water Environ.
783 Res., 90, 840-850. https://doi.org/10.2175/106143017X15131012188006

784 Li, R., Teng, W., Li, Y., Yin, J., Zhang, Z., 2019. Transformation of Phosphorus and Stabilization of Heavy
785 Metals During Sewage Sludge Incineration: The Effect of Suitable Additives and Temperatures. Environ.
786 Sci. Pollut. Res. Int., 26: 29917-29929. https://doi.org/10.1007/s11356-019-06146-2

787 Liu, Y., Shi, H., Li, W., Hou, Y., He, M., 2011. Inhibition of Chemical Dose in Biological Phosphorus and
788 Nitrogen Removal in Simultaneous Chemical Precipitation for Phosphorus Removal. Bioresour. Technol.,
789 102, 4008-4012. https://doi.org/10.1016/j.biortech.2010.11.107

790 Liu, Z., Cichocki, N., Bonk, F., Günther, S., Schattenberg, F., Harms, H., Centler, F., Müller, S., 2018.
791 Ecological Stability Properties of Microbial Communities Assessed by Flow Cytometry. mSphere, 3(1),
792 e00564-17. DOI: 10.1128/mSphere.00564-1

793 Liu, Z., Cichocki, N., Hübschmann, T., Süring, C., Ofiţeru, I.D., Sloan, W.T., Grimm, V., Müller, S., 2019.
794 Neutral Mechanisms and Niche Differentiation in Steady-State Insular Microbial Communities Revealed
795 by Single Cell Analysis. Environ. Microbiol., 21, 164-181. https://doi.org/10.1111/1462-2920.14437

796 Ma, H.Y., Zhang, Y.L., Xue, Y., Li, Y.Y., 2018. A New Process for Simultaneous Nitrogen Removal and
797 Phosphorus Recovery Using an Anammox Expanded Bed Reactor. Bioresour. Technol., 267, 201-208.
798 https://doi.org/10.1016/j.biortech.2018.07.044

799 Macherey-Nagel., Water Analysis - Basic Principle of Water Analysis, in: Schneider, E. (Ed.), Basic Principle
800 of Water Analysis. Macherey-Nagel GmbH & Co. KG, Düren, Germany, p.p. 49

801 Mehr, J., Jedelhauser, M., Binder, C.R., 2018. Transition of the Swiss Phosphorus System Towards a
802 Circular Economy - Part 1: Current State and Historical Developments. Sustainability, 10(5), 1479-1479.
803 https://doi.org/10.3390/su10051479

Mukherjee, C., Chowdhury, R., Begam, M.M., Ganguli, S., Basak, R., Chaudhuri, B., Ray, K., 2019. Effect of Varying Nitrate Concentrations on Denitrifying Phosphorus Uptake by DPAOs with a Molecular Insight Into Pho Regulon Gene Expression. Front. Microbiol., 10. https://doi.org/10.3389/fmicb.2019.02586

Nattorp, A., Remmen, K., Remy, C., 2017. Cost Assessment of Different Routes for Phosphorus Recovery from Wastewater Using Data from Pilot and Production Plants. Water. Sci. Technol., 76(2), 413-424. https://doi.org/10.2166/wst.2017.212

Numberger, D., Ganzert, L., Zoccarato, L., Mühldorfer, K., Sauer, S., Grossart, H.P., Greenwood, A.D., 2019. Characterization of Bacterial Communities in Wastewater with Enhanced Taxonomic Resolution by Full-length 16S rRNA Sequencing. Sci. Rep., 9, 9673. https://doi.org/10.1038/s41598-019-46015-z

Oksanen, J., Blanchet, F.G., Kindt, R., Legendre, P., Minchin, P., O'Hara, B., Simpson, G.L., Solymos, P., Stevens, H.M.H., Syoecs, E. Wagner, H., 2015. Vegan: Community Ecology Package. R Package Version 2.2-1 2015; 2: 1-2.

Orfanos, A.G., Manariotis, I.D., 2019. Algal Biofilm Ponds for Polishing Secondary Effluent and Resource Recovery. J. Appl. Phycol., 31, 1765-1772. https://doi.org/10.1007/s10811-018-1731-8

Otterpohl, R., Freund, M., 1992. Dynamic Models for Clarifiers of Activated Sludge Plants with Dry and Wet Weather Flows. Water Sci. Technol., 26, 1391-1400. https://doi.org/10.2166/wst.1992.0582

Paul, E., Laval, M.L., Sperandio, M., 2001. Excess Sludge Production and Costs Due to Phosphorus Removal. Environ. Technol., 22, 1363-71. https://doi.org/10.1080/09593332208618195

Paula, F.S., Chin, J.P., Schnürer, A., Müller, B., Manesiotis, P., Waters, N., Machintosh, K.A., Quinn, J.P., Connolly, J., Abram, F., McGrath, J.W., O´Flahery V., 2019. The Potential for Polyphosphate Metabolism in Archaea and Anaerobic Polyphosphate Formation in Methanosarcina mazei. Sci. Rep., 9, 17101. https://doi.org/10.1038/s41598-019-53168-4

Peirce, J.J., Weiner, R.F., Vesilind, P.A., 1998. Chapter 9 - Sludge Treatment, Utilization, and Disposal, in: Peirce, J.J., Weiner, R.F., Vesilind, P.A., (Eds.), Environmental Pollution and Control (Fourth Edition). Butterworth-Heinemann, Woburn, pp. 125-135. https://doi.org/10.1016/B978-075069899-3/50010-9

Petzet, S., Cornel, P., 2013. Phosphorus Recovery from Wastewater, in: Hester, R.E., Harrison, R.M., (Eds.), Waste as a Resource. RSC Publishing, London, pp. 110-143. https://doi.org/10.1039/9781849737883-00110

RCoreTeam., 2018. R: A Language and Environment for Statistical Computing. R Foundation for Statistical Computing, Vienna, Austria

Roy, E.D., 2017. Phosphorus Recovery and Recycling with Ecological Engineering: A Review. Ecol. Eng., 98, 213-227. https://doi.org/10.1016/j.ecoleng.2016.10.076

Saunders, A.M., Albertsen, M., Vollertsen, J., Nielsen, P.H., 2016. The Activated Sludge Ecosystem Contains a Core Community of Abundant Organisms. ISME j., 10, 11-20. https://doi.org/10.1038/ismej.2015.117

838 Schönberg, A., Raupenstrauch, H., Ponak, C., 2018. Recovery of Phosphorus in Sewage Sludge Treatment,
839 in: Thiel, S., Thomé-Kozmiensky, E., Winter, F., Juchelková, D., (Eds.), Waste Management, Volume 8,
840 Waste to Energy, Thome-Kozmiensky Verlag Gmbg, Neuruppin p.p. 395-405. ISBN 978-3-944310-42-8

841 Shaddel, S., Bakhtiary-Davijany, H., Kabbe, C., Dadgar, F., Østerhus, S.W., 2019. Sustainable Sewage Sludge
842 Management: From Current Practices to Emerging Nutrient Recovery Technologies. Sustainability, 11,
843 3435. https://doi.org/10.3390/su11123435

844 Sharma, S.B., Sayyed, R.Z., Trivedi, M.H., Gobi, T.A., 2013. Phosphate Solubilizing Microbes: Sustainable
845 Approach for Managing Phosphorus Deficiency in Agricultural Soils. SpringerPlus, 2, 587.
846 https://doi.org/10.1186/2193-1801-2-587

847 Smol, M., 2019. The Importance of Sustainable Phosphorus Management in the Circular Economy (CE)
848 Model: The Polish Case Study. J. Mater. Cycles Waste Manag., 21, 227-238.
849 https://doi.org/10.1007/s10163-018-0794-6

850 Spellman, F.R., 1996. Wastewater Biosolids to Compost. United States, Bosa Roca, p.p. 72. ISBN
851 9781566764612

852 Tarayre, C., de Clercq, L., Charlier, R., Michels, E., Meers, E., Camargo-Valero, M., Delvigne, F., 2016. New
853 Perspectives for the Design of Sustainable Bioprocesses for Phosphorus Recovery From Waste. Bioresour.
854 Technol., 206, 264-274. https://doi.org/10.1016/j.biortech.2016.01.091

855 Tejaswini, E., Babu, G.U., Rao, A.S., 2019. Effect of Temperature on Effluent Quality in a Biological
856 Wastewater Treatment Process. Chemical Product and Process Modeling, 15.
857 https://doi.org/10.1515/cppm-2019-0018

858 Torri, S.I., Correa, R.S., Renella, G., 2017. Biosolid Application to Agricultural Land—a Contribution to
859 Global Phosphorus Recycle: A Review. Pedosphere, 27, 1-16. https://doi.org/10.1016/S1002-
860 0160(15)60106-0

861 Walker, J., 2017. MarketMap - Beating the burn rate for resource and energy recovery from sludge. Global
862 Water Intelligence Magazine, 1, 40–47.

863 Wells, G.F., Wu, C.H., Piceno, Y.M., Eggleston, B., Brodie, E.L., Desantis, T.Z., Andersen, G.L., Hazen, T.C.,
864 Francis, C.A., Criddle, C.S., 2014. Microbial Biogeography Across a Full-Scale Wastewater Treatment Plant
865 Transect: Evidence for Immigration Between Coupled Processes. Appl. Microbiol. Biotechnol., 98, 4723-
866 4736. https://doi.org/10.1007/s00253-014-5564-3

867 Wickham, H., 2016. ggplot2: Elegant Graphics for Data Analysis. Springer-Verlag, New York.
868 https://doi.org/10.1007/978-3-319-24277-4

869 Wilfert, P., Kumar, P.S., Korving, L., Witkamp, G.J., van Loosdrecht, M.C.M., 2015. The Relevance of
870 Phosphorus and Iron Chemistry to the Recovery of Phosphorus from Wastewater: A Review. Environ. Sci.
871 Technol., 49, 9400-9414. https://doi.org/10.1021/acs.est.5b00150

872 Wu, L., Ning, D., Zhang, B., Li, Y., Zhang, P., Shan, X., et al., 2019. Global Diversity and Biogeography of
873 Bacterial Communities in Wastewater Treatment Plants. Nat. Microbiol., 4:,1183-1195.
874 https://doi.org/10.1038/s41564-019-0426-5

875 Yang, Y., Shi, X., Ballent, W., Mayer, B.K., 2017. Biological Phosphorus Recovery: Review of Current
876 Progress and Future Needs. Water. Environ. Res., 89, 2122-2135.
877 https://doi.org/10.2175/106143017X15054988926424

878 Yilmaz, G., Cetin, E., Bozkurt, U., Magden, K., 2017. Effects of Ferrous Iron on the Performance and
879 Microbial Community in Aerobic Granular Sludge in Relation to Nutrient Removal. Biotechnol. Prog., 33.
880 https://doi.org/10.1002/btpr.2456

881 Zhang, B., Yu, Q., Yan, G., Zhu, H., Xu, X.Y., Zhu, L., 2018. Seasonal Bacterial Community Cuccession in Four
882 Typical Wastewater Treatment Plants: Correlations Between Core Microbes and Process Performance.
883 Sci. Rep., 8, 4566. https://doi.org/10.1038/s41598-018-22683-1

884 Zhang, L., Shen, Z., Fang, W., Gao, G., 2019. Composition of Bacterial Communities in Municipal
885 Wastewater Treatment Plant. Sci. Total Environ., 689, 1181-1191.
886 https://doi.org/10.1016/j.scitotenv.2019.06.432

887 Zhao. J., Liu, X., 2013. Organic and Inorganic Phosphorus Uptake by Bacteria in a Plug-Flow Microcosm.
888 Front. Env. Sci. Eng., 7, 173-184. https://doi.org/10.1007/s11783-013-0494-3

889

890 **FIGURES**

891 **Figure 1**: Scheme of the WWTP Eilenburg process streams. The numbers highlight the sampling points for
892 P determination: 1.inflow, 2.grit chamber start, 3.grit chamber end, 4.primary clarifier, 5.primary sludge,
893 6.aeration tank1, 7.aeration tank2, 8.precipitation shaft, 9.secondary clarifier1, 10.secondary clarifier2,
894 11.return sludge, 12.excess sludge, 13.anaerobic digester sludge, 14.centrate, 15.biosolids, 16.effluent.
895 Wastewater streams are marked by brown arrows, sludge streams are marked by grey arrows, biosolids
896 are marked with black arrow and effluent marked with blue arrow. Sampling points are named according
897 to the WWTP process stages.

898

899 **Figure 2**: Graphical summary of the WWTP P balance with regard to free P, bound P, total P, daily P mass
900 load rates, and P content in DM. The total P mass load rates were weighted against P content in DM. The
901 economically feasible P thresholds for application of P recovery technologies were set for the total P (free
902 and bound P) concentration of 0.05 kg m^{-3} (horizontal red line) and for P content in DM of 20 g P kg_{DM}^{-1}
903 (vertical red line). The value of total P mass load rates is represented by the size of the circles within which
904 the percentages of bound P vs. free P were highlighted. Promising P recovery process streams towards
905 high amounts of total P (free P and bound P) and high daily P mass load rates were visualized by the circles
906 above the red horizontal line. Process streams that have P contents higher than 20 g P kg_{DM}^{-1} were
907 visualized on the right side of the vertical red line.

908

Figure 3: Variation of community structures over 748 days of sampling, visualized by NMDS plotting of the Bray-Curtis distance measure. The cytometric data were evaluated with the tool flowCybar. All 16 individual sampling points are shown. Each circle represents a community and the size of each circle corresponds to the time of sampling, starting with day 1 as the smallest circle. The centroids are marked with a black cross. The average distance to centroid (DTC) within each community is shown on the lower left side of each plot and the centroid coordinates in SI Table 5. 1.inflow, 2.grit chamber start, 3.grit chamber end, 4.primary clarifier, 5.primary sludge, 6.aeration tank1, 7.aeration tank2, 8.precipitation shaft, 9.secondary clarifier1, 10.secondary clarifier2, 11.return sludge, 12.excess sludge, 13.anaerobic digester sludge, 14.centrate, 15.biosolids, 16.effluent.

Figure 4: Circos plot representing the interactions between microbial SCs and concentrations of bound and free P based on Spearmans correlation coefficient rho, which was calculated by successive addition of sampled days per process stream until the end of the sampling campaign. Correlations are given as colored lines between the color coded sampling points and the respective P type (red: positive correlations, grey: negative correlations). The axis indicates the number of all significant correlations (P<0.05) per process stream corrected by the number of days and the number of SCs with at least 1% average relative cell abundance (SCs = nr.gate). Only sampling points with economically feasible concentrations of bound P and free P were included in the analysis (5.primary sludge, 6. and 7.aeration tank1,2, 11.return sludge, 12.excess sludge, 13.anaerobic digester sludge, 14.centrate, 15.biosolids). For the microbial communities data obtained with the tool flowCyBar were used for the analysis. Additional information can be found in the corresponding heatmaps (SI Figure 5).

Figure 5: Circos plot representing the interactions between microbial SCs and concentrations of biologically bound P and free P for either days with rather chemically removed P (upper 25% quintile: 15.65 kg d^{-1}P; left side) or days with rather biologically removed P (upper 25% quintile: 36.28 kg d^{-1} P; right side), indicating times with inefficient and efficient biological P removal. Spearmans correlation coefficient rho and successive addition of the data of the sampling points was used for the correlation analysis. Colored lines between the color coded sampling points and the respective P type highlight the type of interactions. The axis indicates the number of all significant correlations (P<0.05) per process stream corrected by the number of days and the number of SCs with at least 1% average relative cell abundance (SCs = nr.gate). Sampling points 6. and 7.aeration tank1,2, 8.precipitation shaft, 11.return sludge,

12.excess sludge, 13.anaerobic digester sludge, 14.centrate, and 15.biosolids were investigated. Additional information can be found in SI Figure 3 and corresponding heatmaps (SI Figure 6).

Figure 1

Click here to access/download;Figure;Figure 1.pdf

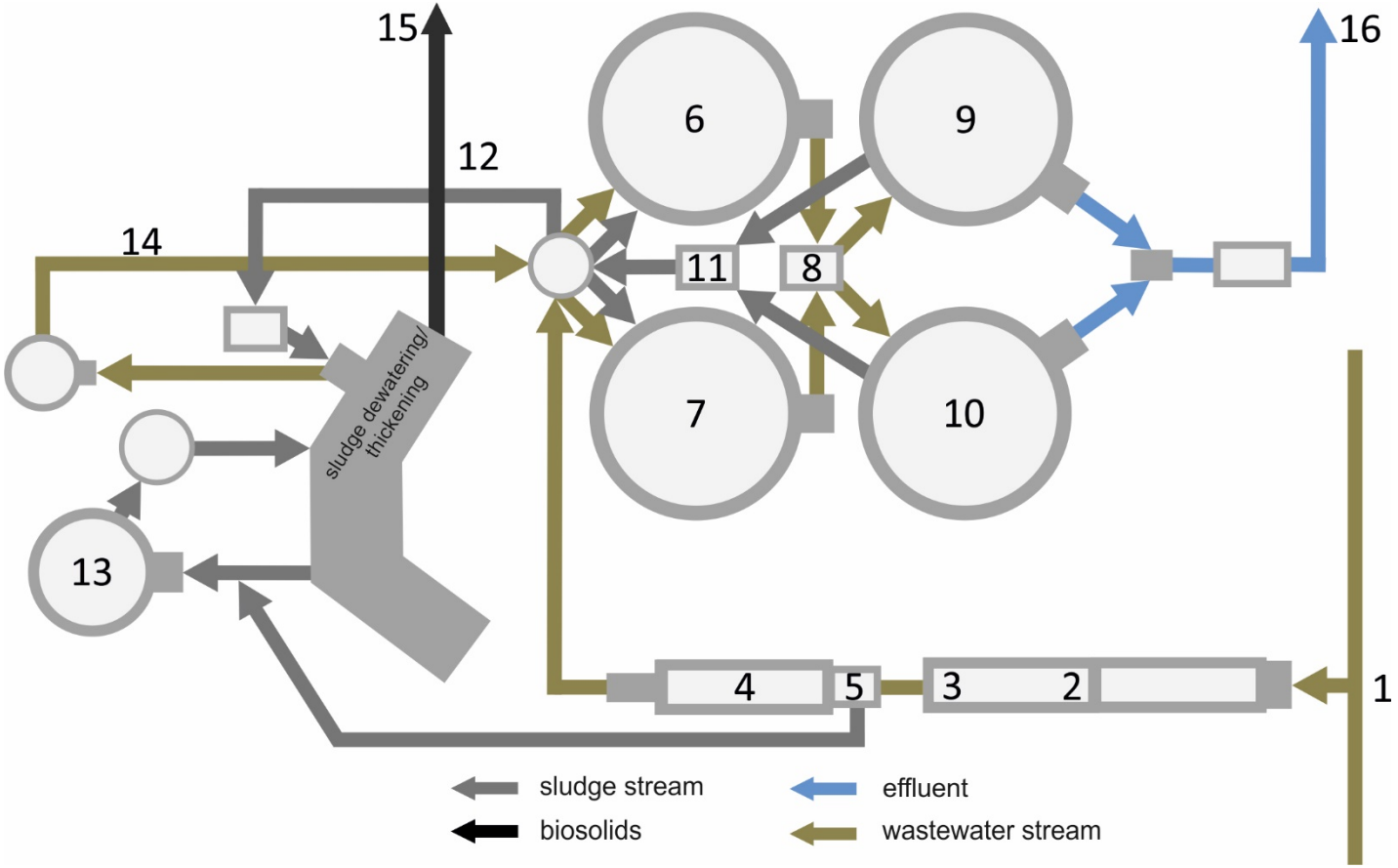

Figure 2

Click here to access/download;Figure;Figure 2.pdf

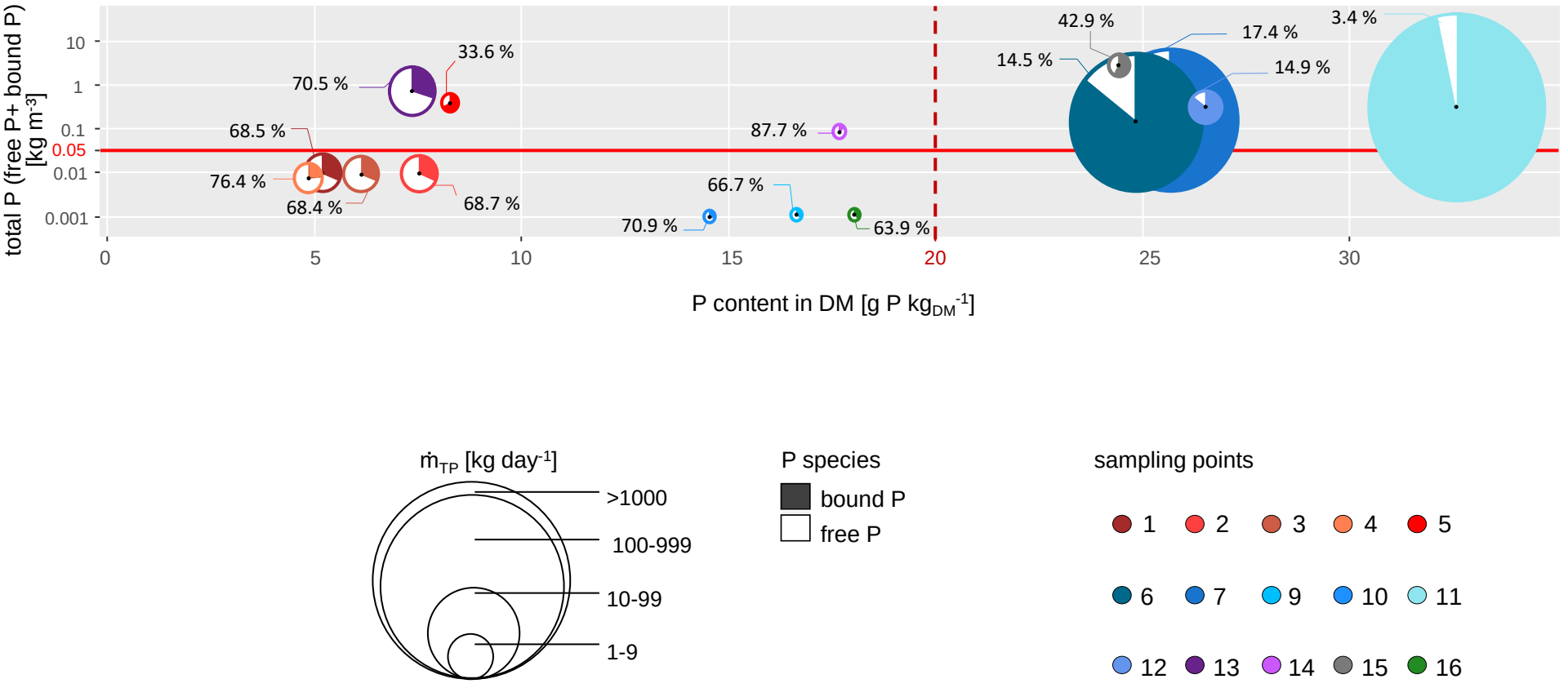

Figure 3

Click here to access/download;Figure;Figure 3.pdf

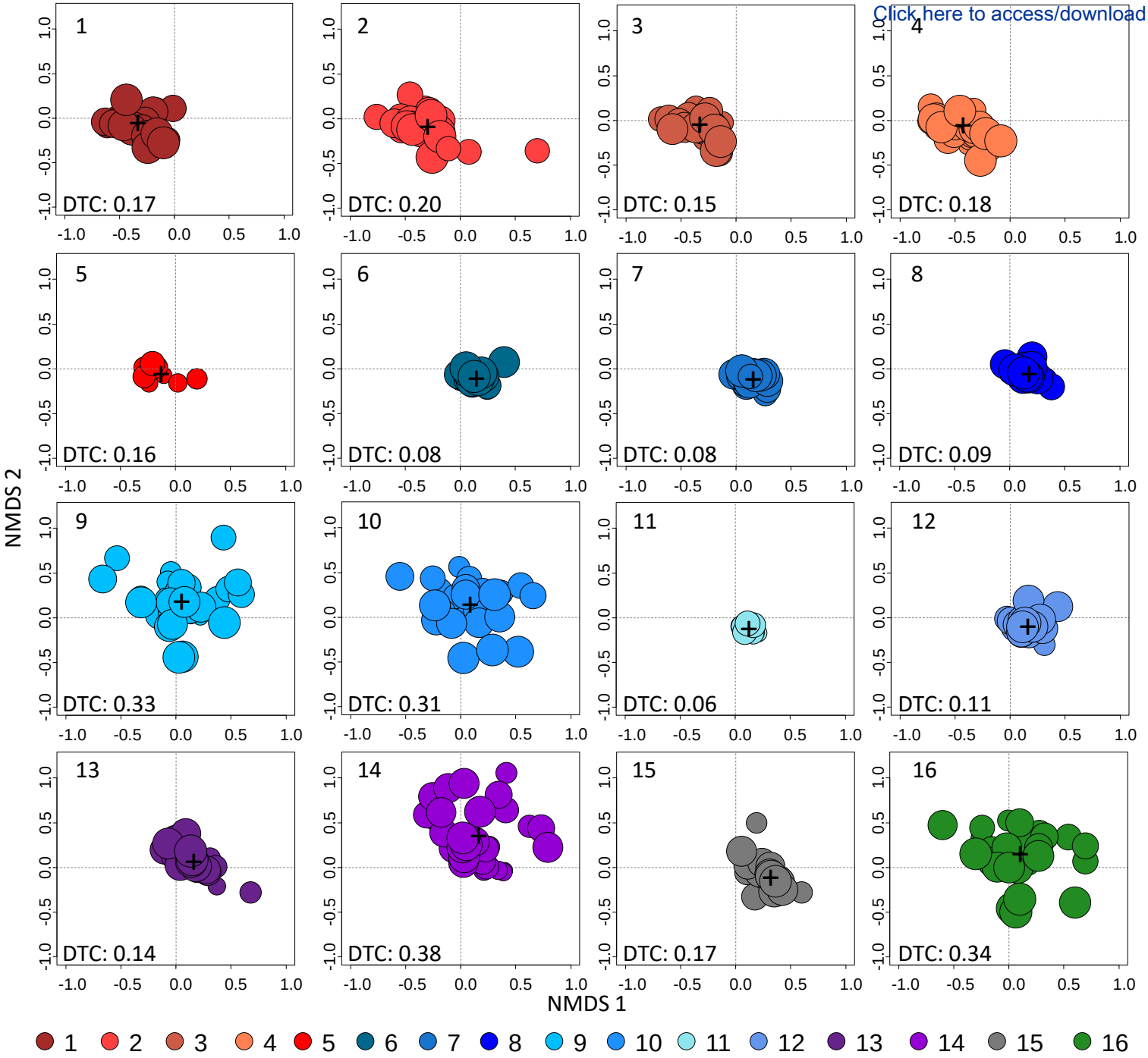

Figure 4

Click here to access/download;Figure;Figure 4.pdf

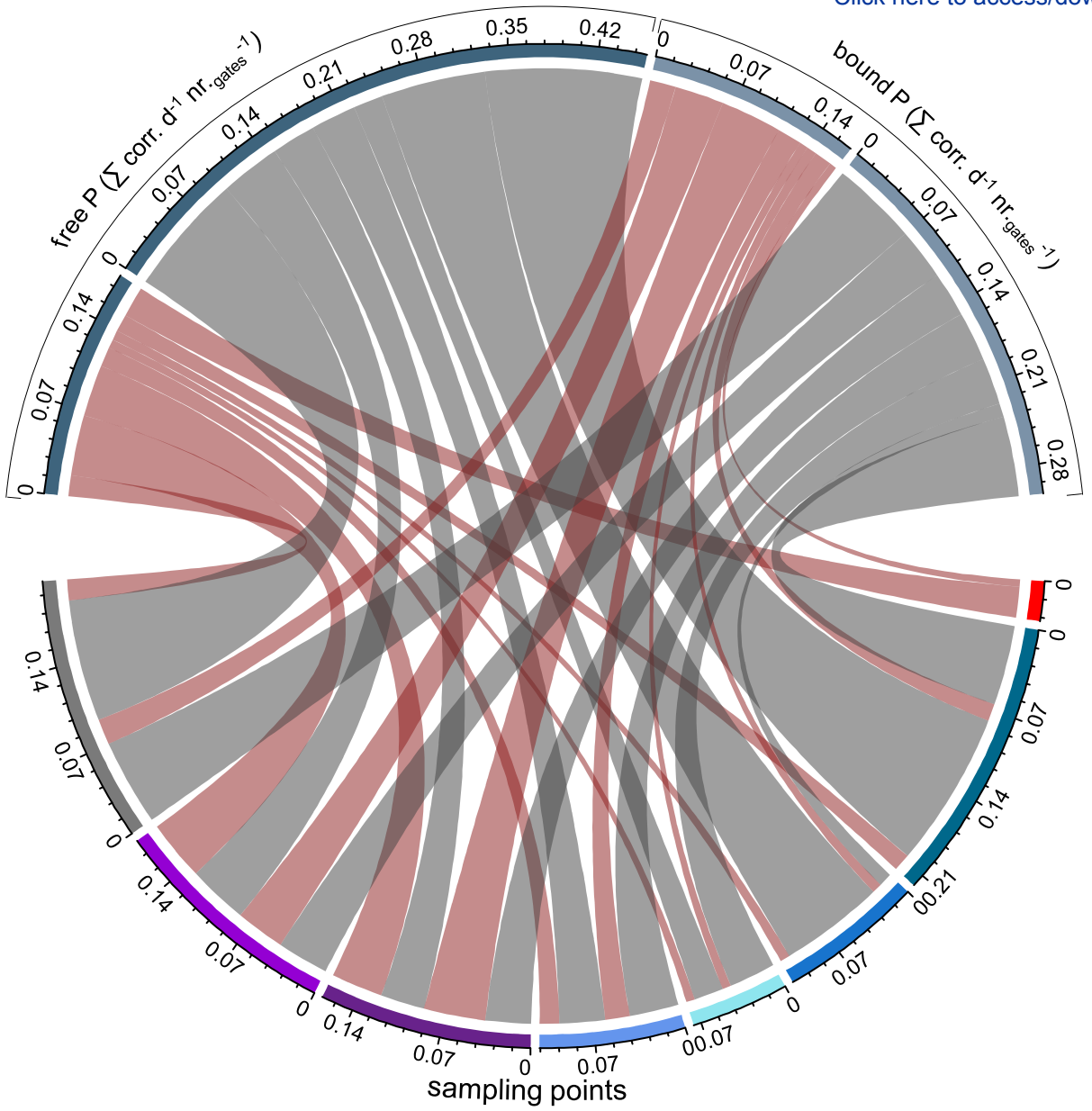

Figure 5

Click here to access/download;Figure;Figure 5.pdf

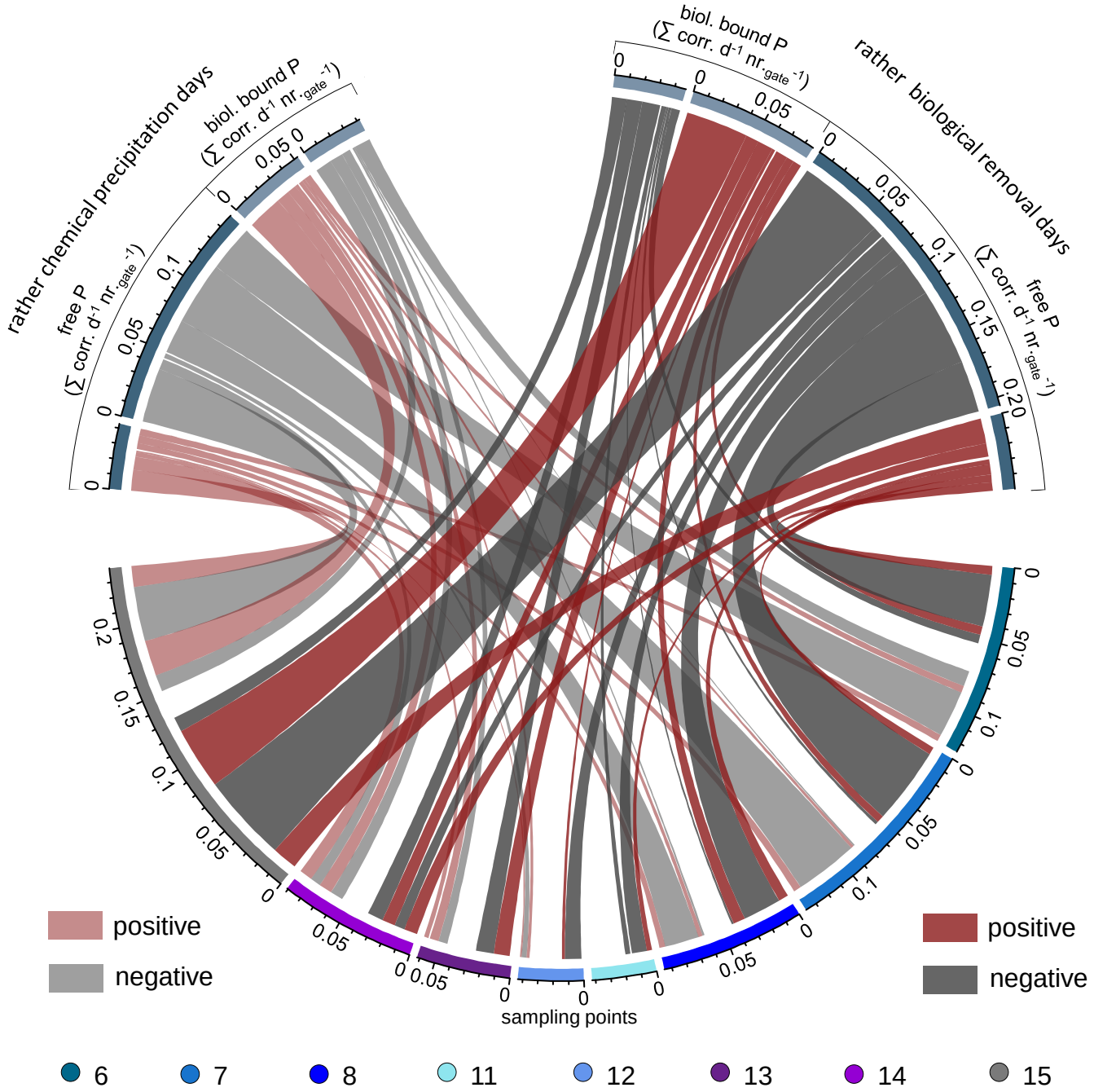

SI Figures all-line publication only

SI Tables all-line publication only

AUTHOR CONTRIBUTIONS

VV: conceptualization, methodology, framework of P-cycle assessment, calculation and evaluation of data, validation of data, writing; CS: sampling, methodology, flow cytometry; HH: reviewing, editing; SM: conceptualization, writing, reviewing, editing; SG: data curation, visualization, reviewing, editing.

DECLARATION OF INTEREST

The authors have no competing interests to declare.